Automatic Polyp Detection using DSC Edge Detector and HOG Features

Himanshu Agrahari[1], Yuji Iwahori[2], M. K. Bhuyan[1], Somnath Ghorai[1], Himanshu Kohli[1], Robert J. Woodham[3] and Kunio Kasugai[4]

[1]*Dept. of Electronics and Electrical Engineering, Indian Institute of Guwahati, Guwahati 781039, India*

[2]*Dept. of Computer Science, Chubu University, Kasugai 487-8501, Japan*

[3]*Dept. of Computer Science, University of British Columbia, Vancouver V6T 1Z4, Canada*

[4]*Dept. of Gastroenterology, Aichi Medical University, Nagakute 480-1195, Japan*

Keywords: Endoscopy, Discrete Singular Convolution, Histogram of Oriented Gradients (HOG), Conic Fitting, Support Vector Machine.

Abstract: Endoscopy is a very powerful technology to examine the intestinal tract and to detect the presence of any possible abnormalities like polyps, the main cause of cancer. This paper presents an edge based method for polyp detection in endoscopic video images. It utilizes discrete singular convolution (DSC) algorithm for edge detection/segmentation scheme, then by using conic fitting techniques (ellipse and hyperbola) potential candidates are determined. These candidates are first rotated so as to make major axis in the x-axis direction, and then classified as polyp or non-polyp by SVM classifier which is trained separately for ellipse and hyperbola with HOG features.

1 INTRODUCTION

Medicine is an important area of application for computer vision. Endoscopy allows medical practitioners to observe the interior of hollow organs and other body cavities in a minimally invasive way. Diagnosis involves both shape detection and the assessment of tissue state. For example, a polyp is a pathological condition directly related to geometrical shape. Diagnosis typically requires polyp removal and biopsy.

Polyps are abnormal growth of tissues from mucous membrane (Fig.1). An early stage detection and cure can save a human life as it develops into cancer if undetected for a long time. It has been reported that colorectal cancer is the second leading cause of cancer-related deaths in U.S. (Parker and Tong, 1997).

There are some previous approaches to extract polyp candidate region from endoscope image.

Some work has used a patch-based approach (Iakovidis and Maroulis, 2005)-(Alexandre and Nobre, 2008). In (Iakovidis and Maroulis, 2005) and (Karkanis and Iakovidis, 2003), patch features computed are the Color Wavelet Covariance (CWC) and the Local Binary Pattern (LBP). Candidate patches are classified using an SVM. In (Alexandre and Nobre, 2008), higher dimensional features of the RGB color values and the XY position coordinates are used leading to improved classification performance.

Figure 1: Polyp shown inside the yellow circle.

Performance of previous patch-based approaches depends on the patch size. It is not straightforward to detect polyps with differing sizes in an image. Further, smaller polyps become quite sensitive to the features used for detection. It is difficult to imagine how to achieve robustness with a constant patch size.

Paper (Viana and Iwahori, 2013) proposes that Sobel edge extraction technique has been used to detect the edges and then classified the regions as polyp and non-polyp using shape or geometric features like circularity, complexity, diameter etc. using SVM classifier. The presence of a lot of noise in endoscopic

Agrahari H., Iwahori Y., K. Bhuyan M., Ghorai S., Kohli H., J. Woodham R. and Kasugai K..
Automatic Polyp Detection using DSC Edge Detector and HOG Features.
DOI: 10.5220/0004756104950501
In *Proceedings of the 3rd International Conference on Pattern Recognition Applications and Methods* (ICPRAM-2014), pages 495-501
ISBN: 978-989-758-018-5

images results in the failure of typical edge detection techniques such as Sobel.

Log Gabor filter has been used as segmentation scheme (Karargyris and Bourbakis, 2009), in conjunction with the SUSAN edge detector, geometric information was used for classification after segmentation.

Hessian filter was used to find the polyp candidates then HOG features of the candidate regions were computed for each component of the HSV color space (Iwahori and Shinohara, 2013), where SVM is introduced to classify the candidate region extracted by Hessian filter but this Hessian filter costs much time for extracting candidate region with over-detection.

In paper (Hwang and Oh, 2007), only elliptical shape features are considered after edge detection. In many cases, polyp could resemble more to a hyperbola than an ellipse and such cases leads to loss of accuracy.

In this paper, DSC algorithm for edge detection, a special class of DSC kernels as described in paper (Hou and Wei, 2002) is used. Conic fitting is then applied to these edges to find the potential candidates, which are then classified as polyps and non-polyps by a SVM classifier which is trained separately for ellipse and hyperbola with HOG features extracted from DSC filtered images.

Our research is to classify the frames as polyp and non-polyp and finally reducing physician's workload by passing the frames having high probability for polyp.

2 PROPOSED METHOD

The block diagram is shown in Fig.2 and this has been divided into 4 major parts.

2.1 Dataset Preprocessing

2.1.1 Non-linear Filtering

Random variations in brightness or color decreases the sensitivity of any algorithm. To tackle this, image is first passed through non-linear filter like median filter. Here gray scale image is used.

2.1.2 Contrast Enhancement

In order to enhance the visibility of local details in an image, CLAHE (Breckon and Solomon, 2011) is used to improve image contrast. It is usually chosen over simple Histogram Equalization because it can overcome common problems like image saturation and noise amplification.

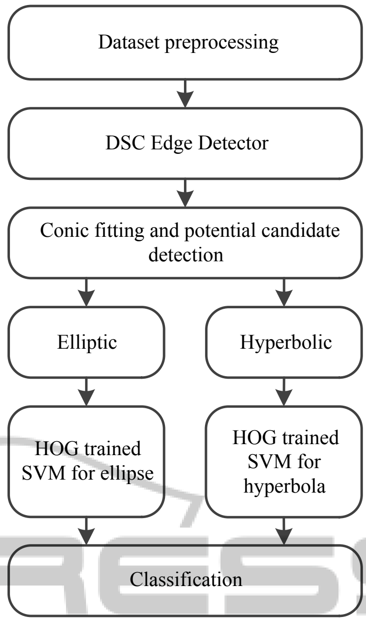

Figure 2: Proposed Block Diagram.

2.1.3 Specularity Removal

A polyp image obtained from conventional endoscope has both specular and diffused components. In medical image processing where details are so minute that it is difficult to extract features, specular regions make the process more difficult and inaccurate which results in loss of needful data. We cannot directly apply our algorithms on these images. As we can see in Fig.3(b), pixels having specularity show high peaks, which eat-up the smooth and round property, which are the basic conditions for our research. The implementation is based on (Shen and Cai, 2009). Specular components are detected and removed, and then interpolation is done, which round off the values to neighboring ones.

Let I be an RGB image with RGB value set per pixel of the form V_R, V_B, V_G . Using these values we define certain terms on per pixel basis.

Terms:

$$V_{min} = min(V_R, V_B, V_G) \tag{1}$$

$$V_{mean} = mean(V_{min}) \tag{2}$$

$$V_{std} = StandardDeviation(V_{min}) \tag{3}$$

$$T_v = V_{mean} + k \times V_{std} \tag{4}$$

where k = 0.5 suits most of the results

Calculation:

Find an offset t_p such that:

$$t_p = T_v \text{ if } V_{min} > T_v \tag{5}$$

$$= V_{min} \text{ else} \tag{6}$$

Find β which determines the specular component as:

$$\beta = V_{min} - t_p \tag{7}$$

$$I_{Specular} = 0.5\beta \tag{8}$$

This specular component calculated is further dilated so that when it is subtracted from the original image it does not give thin high intensity boundaries.

$$I_{SpecularRemoved} = I - binary(I_{Specular}) \tag{9}$$

Now it can be seen this $I_{SpecularRemoved}$ has holes which need to be covered. So holes are filled on the basis of neighboring values. Use a spring metaphor. Assumes springs (with a nominal length of zero) connect each node with every neighbor (horizontally, vertically and diagonally) since each node tries to be like its neighbors,extrapolation is as a constant function where this is consistent with the neighboring nodes. As a result, specular removed leveled image is generated.

2.2 DSC Edge Detector

In this method, Discrete Singular Convolution (DSC) for edge detection using particular class of DSC kernels as described in (Hou and Wei, 2002) has been used. To construct edge detectors, one dimensional, n-th order DSC kernel of delta type is used:

$$\delta^{(n)}_{\sigma,\alpha}(x - x_k), n = 0, 1, 2, \cdots \tag{10}$$

where

$$\delta_{\sigma,\alpha} = \frac{\sin(\alpha)(x - x_k)}{(\alpha)(x - x_k)} e^{-(x-x_k)^2/2\sigma^2} \quad (\sigma > 0) \tag{11}$$

$$\delta_\alpha(x) = \frac{\sin(\alpha x)}{\pi x} \tag{12}$$

and the superscript denotes the n-th order derivative.

Now $\delta_\alpha(x)$ is nothing but Shannon's delta kernel which corresponds to a family of ideal low pass filters, each having different bandwidth. Their corresponding wavelet expressions $\psi_\alpha(x)$ are band pass filters.

$$\psi_\alpha(x) = \frac{\sin 2\alpha x - \sin \alpha x}{\pi x} \tag{13}$$

The Fourier transformation of $\delta_\alpha(x)$ and $\psi_\alpha(x)$ are not differentiable so a regularization procedure is used and the resulting DSC kernel in its discretized form is

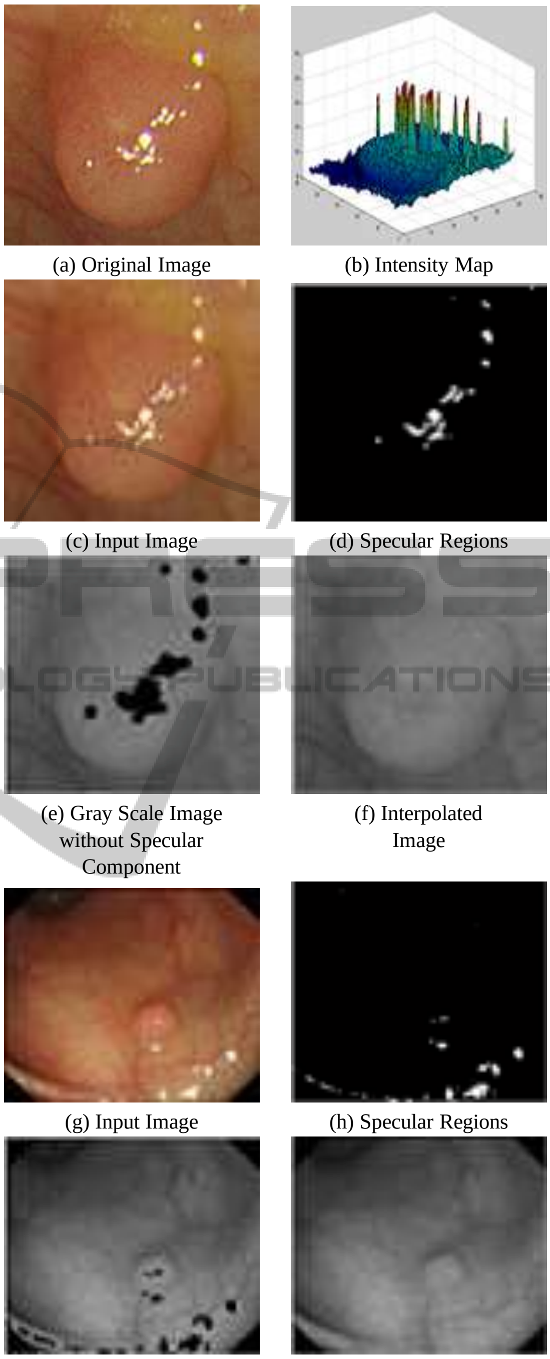

(a) Original Image (b) Intensity Map

(c) Input Image (d) Specular Regions

(e) Gray Scale Image without Specular Component (f) Interpolated Image

(g) Input Image (h) Specular Regions

(i) Gray Scale Image without Specular Component (j) Interpolated Image

Figure 3: Specularity Removal.

expressed as $\delta_{\alpha,\pi}(x)$ whose Fourier transform is infinitely differentiable. . The derivatives $\delta^{(n)}_{\sigma,\alpha}(x_m - x_k)$ (n=1,2,$\cdots$) are obtained by differentiation and can be regarded as high pass or band pass filters depending upon the value of the parameters. In this paper, the first order derivatives have been used and these regularized filters are functions of Schwartz class which have controlled residue amplitude at large values of x.

Fig.4 (a) illustrates the impact of parameter σ on the filter in the frequency domain for a fixed value of α. With the increase in value of σ the filter becomes more localized in frequency domain and in time domain larger the value of σ, slower the filter will decay. Fig.4 (b) shows the impact of α on the frequency response of first order derivative for a fixed σ. Increasing the value of α moves the peak of frequency response from the low frequency region to the higher. So by balancing the values of σ and α in accordance with the practical problem good results can be obtained for example in case of high noise corruption smaller values of α can be used. In case of polyp detection in endoscopic images, the edge definition is not very sharp as polyp and their neighboring areas are similar in texture and there is a lot of noise in images so smaller values of α and σ should be used so as to localize the frequency response at near about mid frequency range.

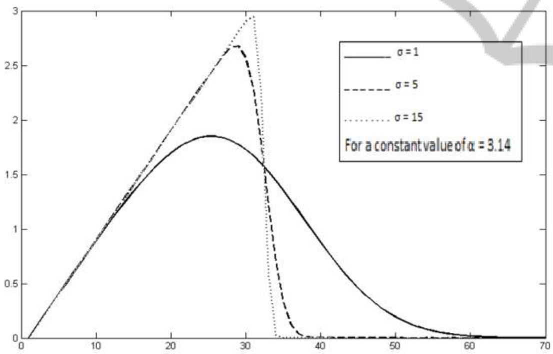

(a) $\delta^{(1)}_{\sigma,\alpha}(x)$ for different values of σ

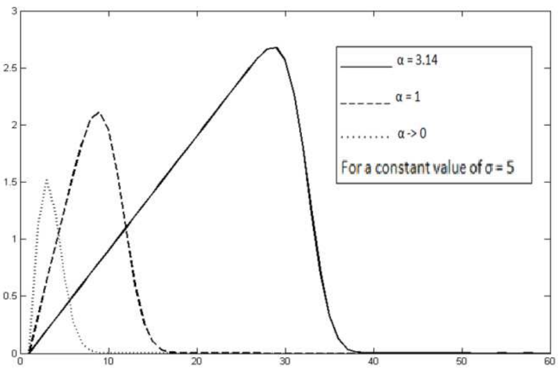

(b) $\delta^{(1)}_{\sigma,\alpha}(x)$ for different values of α

Figure 4: Frequency response of $\delta^{(1)}_{\sigma,\alpha}(x)$.

The 1st order fine scale DSC Edge Detector (DSCED) is given by

$$DSCED^1(x_i,x_j) = \left|\sum_{k=-W_n}^{W_n} \delta^{(1)}_{(\sigma,\alpha)}(x_i - x_k) I(x_k,y_j)\right| + \left|\sum_{l=-W_n}^{W_n} \delta^{(1)}_{(\sigma,\alpha)}(y_j - y_l) I(x_i,y_l)\right| \quad (14)$$

where $I(x,y)$ is the intensity of input image.

Fig.5 shows a comparison between DSC filter and Sobel operator. Before applying curve fitting technique, noises have to be removed. In case of typical edge detection techniques (Sobel in this case) detected polyp boundaries are also similar to noise as in Fig.5(a) and (c). Noise elimination results in the elimination of polyp boundaries but not in case of DSC. In some cases as in Fig.5(e) and (g), the polyp boundaries are not even detected in case of Sobel but are detected well with DSC.

2.3 Conic Fitting and Potential Candidate Detection

The extracted edges are of different sizes and orientations. So the polyp could be a single edge or as a part of a big edge (as shown in Fig.6 (b) green patch). Both the cases are considered by uniformly picking random points within a connected edge. The number of points is proportional to the length of the connected component. Connected components with size greater than a particular threshold are only considered. Now for every picked point a square patch (160x160 pixels) is drawn around it with the point at the center. Fig.6 (b) shows some of them. Now this square patch is checked for which conic it represents better. The process is performed on the basis of least square fit.

Fig.7 (b) and (d) show ellipse and hyperbola fit respectively. Dividing this into class increases the classifier accuracy. All the geometric parameters (major axis, minor axis, center, orientation angle) are calculated. The conic which satisfy the following condition:

$$(Majoraxis/Minoraxis) \leq 2 \quad (15)$$

are selected as potential candidates (in Fig.6 (b), B is selected, but A and C are rejected) and are saved in the respective groups of ellipse and hyperbola along with data of orientation angle (which is used at the time of classification).

2.4 HOG Feature Extraction and SVM Classification

HOG Feature Extraction:

Patches finally obtained are rotated so as to bring the major axis orientation to zero. Fig.7 (b) and (d) show the rotated images. The HOG (Dalal and Triggs,

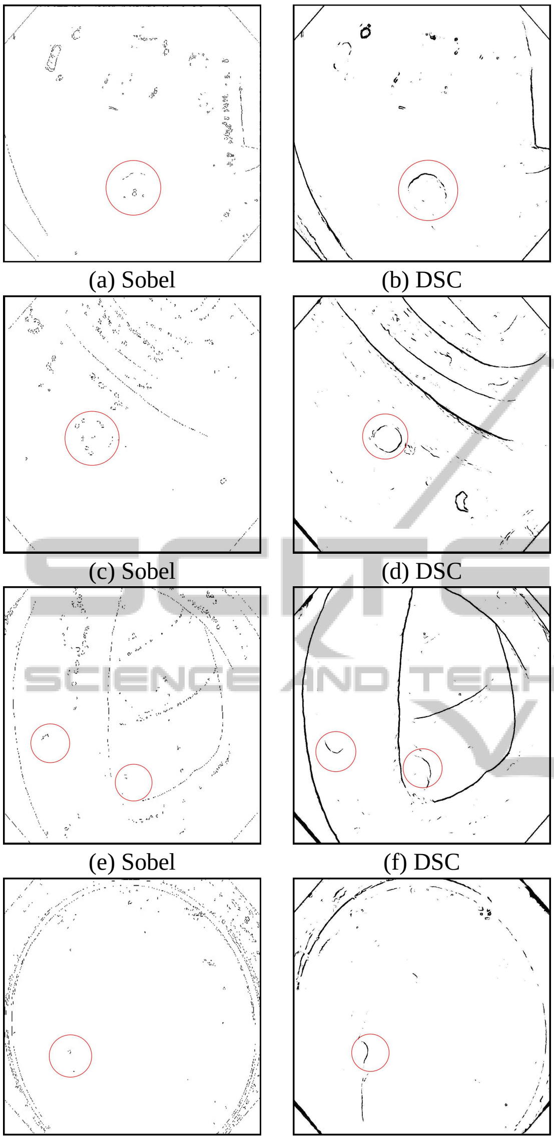

(a) Sobel (b) DSC (c) Sobel (d) DSC (e) Sobel (f) DSC (g) Sobel (h) DSC

Figure 5: Result of Edge Map.

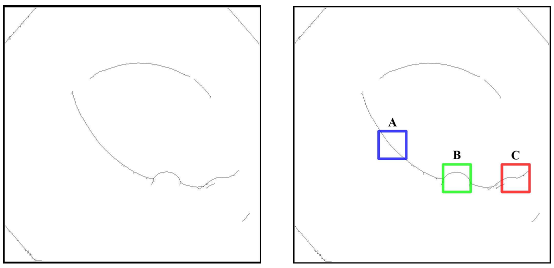

(a) Edge map of polyp image (b) uniformly selected square patches

Figure 6: Square Patches.

2005) feature vectors are calculated. Rotation increases the sensitivity of HOG features.

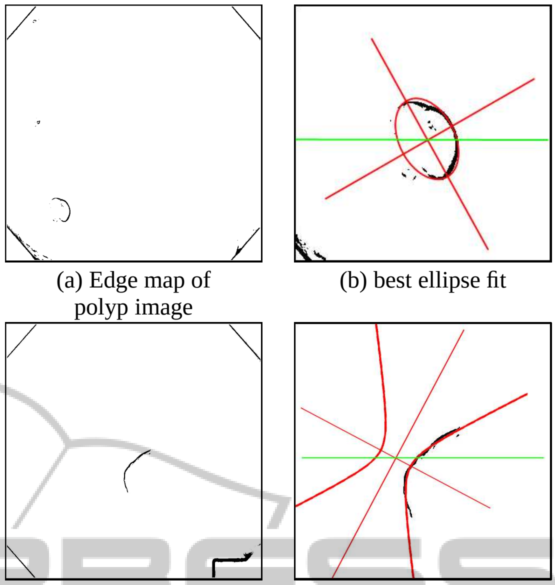

(a) Edge map of polyp image (b) best ellipse fit (c) Edge map of polyp image (d) best hyperbola fit

Figure 7: Best Conic Fit.

Classification:

Support Vector Machine is used for classification. The radial basis function (RBF) kernel type was used, as expressed by the equation below:

$$K(x,x') = e^{-\frac{\|x-x'\|^2}{2\sigma^2}} \tag{16}$$

x and x' are two samples and σ is inversely proportional to kernel width. SVM was trained separately for Ellipse and Hyperbola. 140 positive images, 176 negative images for ellipse and 186 positive images, 286 negative images for hyperbola were used to train the SVM. Each image was of 160 $\times$ 160 pixels. The dimensionality of the resulting HOG feature vector was 168. The patches corresponding to ellipse and hyperbola are classified separately with doubly trained SVM.

3 EXPERIMENTAL RESULTS

In this section, we assess the effectiveness of the proposed method using the set of 87 endoscopic images taken from various patients. The set contains 50 polyp images and 37 non-polyp images each of resolution 1000x1000 pixels. The images are first preprocessed then gray scaled images are passed through DSC filter. We tried different combinations of (α, σ) values like (0.4,1), (0.4,3), (0.8,1), (0.8,3), (1.5,1), (1.5,3) and different widths 3,5,7,9 and out of these α=0.4, σ=1 and width=9 were chosen by analyzing the time complexity and the quality of edges obtained. The DSC filtered image is then thresholded so as to get a binary image. The threshold in this case is empirically determined as 8. A green circle is drawn when a section of an edge is classified as polyp. In case of polyp edges many intersecting circles are drawn in close vicinity, because of selection of uniformly distributed random points for conic fitting mentioned in the previous section. So we adopt a voting method. In case of non intersecting circles, votes are not been recorded. To get a polyp detected two or more circles should intersect. Single circle vote is not counted.

Fig.8 show the original endoscopic images, with green circles marked at the area where polyp has been detected.

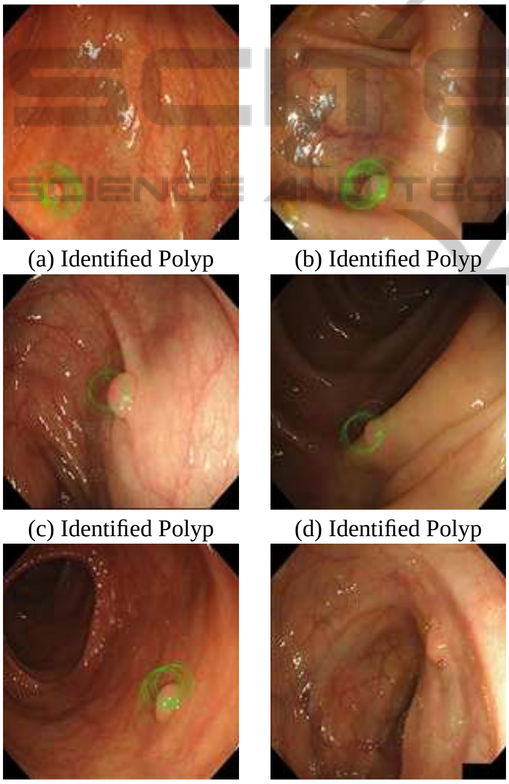

(a) Identified Polyp (b) Identified Polyp (c) Identified Polyp (d) Identified Polyp (e) Identified Polyp (f) Missed Polyp because of single vote

Figure 8: Polyp Detection.

Accuracy, sensitivity and specificity are given in Table 1.

4 CONCLUSIONS

In this paper a novel method for polyp detection has been presented combining DSC edge detection with conic fitting (both ellipse and hyperbola) technique. Classification is based on HOG features from DSC filtered images. The power of the methodology lies in the DSC edge detection technique. Proposed edge detection is focused on the idea that due to the possible presence of noise, the definition of image edge is not sharp so finding edge by gradient methods becomes an ill-posed problem. In case of endoscopic images, the sources of noise are a lot, whether it is specularity, blood vessels or saliva. Another problem lies in the similarities of texture between polyp and its surrounding regions. The DSC edge detection technique is able to deal with these two problems which is clear from experimental results and its comparison with Sobel.

Results also show the advantage of including hyperbola with ellipse in conic fitting. Extracting HOG features from DSC filtered images instead of original image have resulted in higher accuracy after SVM classification.

The experimental results shows that the overall methodology is quite promising and future work should be extended to video sequences to perform real-time detection.

Table 1: Classification Performance.

Method	Accuracy	Sensitivity	Specificity
Only ellipse fitting with HOG over DSC*	52.87 %	74.00 %	24.32 %
Ellipse and hyperbola fitting with HOG over original gray scale image	50.57%	74.00 %	18.92%
(Proposed) Ellipse and hyperbola fitting with HOG over DSC*	89.65 %	90.00 %	89.18 %

ACKNOWLEDGEMENTS

This research was done while Himanshu Agrahari visited Iwahori Lab. for his research internship and they did B.Tech project at IIT Guwahati as the research collaboration. Iwahori's research is supported by Japan Society for the Promotion of Science (JSPS) Grant-in-Aid for Scientific Research (C) (23500228) and Chubu University Grant. Woodham's research is supported by the Natural Sciences and Engineering

Research Council (NSERC).

REFERENCES

Alexandre, L. and Nobre, N. (2008). Color and position versus texture features for endoscopic polyp detection. In *Int. Conf. on BioMedical Engineering and Informatics (BMEI), Vol.2, pp.38-42*. IEEE.

Breckon, T. and Solomon, C. (2011). Fundamentals of digital image processing: a practical approach with examples in matlab. In *Wiley-Blackwell, pp.76-79*.

Dalal, N. and Triggs, B. (2005). Histograms of oriented gradients for human detection. In *IEEE CVPR, Vol.1, pp.886-893*.

Hou, Z. and Wei, G. (2002). A new approach to edge detection. In *Pattern Recognition 35 (7), pp.1559-1570*.

Hwang, S. and Oh, J. (2007). Polyp detection in colonoscopy video using elliptical shape feature. In *Proc. of the Int. Conf. on Image Proc., pp. II-465 - II-468*.

Iakovidis, D. and Maroulis, D. (2005). A comparative study of texture features for the discrimination of gastric polyps in endoscopic video. In *18th IEEE Symposium on Computer-Based Medical Systems, Vol.7, No.3, pp.141-152*. IEEE.

Iwahori, Y. and Shinohara, T. (2013). Automatic polyp detection using hessian filter. In *IAPR MVA2013, Health and Life, 3-1, pp.21-247*.

Karargyris, A. and Bourbakis, N. (2009). Identification of polyps in wireless capsule endoscopy videos using log gabor filters. In *LiSSA, pp.143-147*. LiSSA.

Karkanis, S. and Iakovidis, D. (2003). Computer-aided tumor detection in endoscopic video using color wavelet features. In *IEEE Trans. on Information Technology in Biomedicine*. IEEE.

Parker, S. and Tong, T. (1997). Cancer statistics 1997. In *CA Cancer J. Clinicians, Vol.47, pp.5-27*. Wiley.

Shen, H. and Cai, Q. (2009). Simple and efficient method for specularity removal in an image. In *Applied Optics, 48(14), pp.2711-2719*.

Viana, R. and Iwahori, Y. (2013). Automated polyp image extraction from endoscope images. In *International Workshop on Advanced Image Technology (IWAIT2013), pp.216-221*. IWAIT.